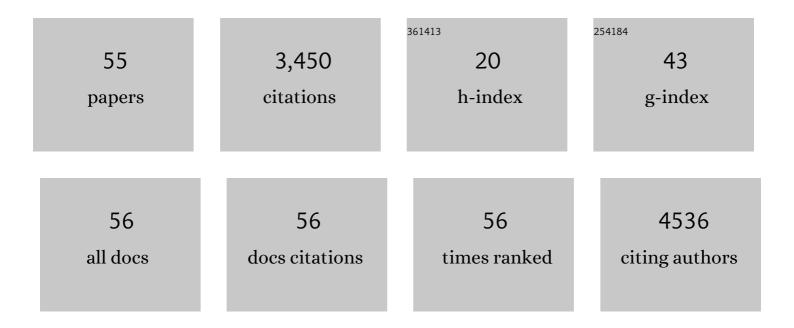
Eugenio Cantatore

List of Publications by Year in descending order

Source: https://exaly.com/author-pdf/7011467/publications.pdf Version: 2024-02-01



#	Article	IF	CITATIONS
1	A 0.32 nW–1.07 µW All-Dynamic Versatile Resistive Sensor Interface With System-Level Ratiometric Measurement. IEEE Transactions on Circuits and Systems I: Regular Papers, 2022, 69, 506-517.	5.4	3
2	A 103-dB SFDR Calibration-Free Oversampled SAR ADC With Mismatch Error Shaping and Pre-Comparison Techniques. IEEE Journal of Solid-State Circuits, 2022, 57, 734-744.	5.4	12
3	A Prototype System With Custom-Designed RX ICs for Contrast-Enhanced Ultrasound Imaging. IEEE Transactions on Ultrasonics, Ferroelectrics, and Frequency Control, 2022, 69, 1649-1660.	3.0	1
4	A Compact 0.0054 mm ² Multipurpose Analog Frontend for Ultrasound Digitizers in 40nm CMOS. IEEE Transactions on Circuits and Systems II: Express Briefs, 2022, 69, 2483-2487.	3.0	1
5	A 7.3-μ W 13-ENOB 98-dB SFDR Noise-Shaping SAR ADC With Duty-Cycled Amplifier and Mismatch Error Shaping. IEEE Journal of Solid-State Circuits, 2022, 57, 2078-2089.	5.4	9
6	A printed proximity-sensing surface based on organic pyroelectric sensors and organic thin-film transistor electronics. Nature Electronics, 2022, 5, 289-299.	26.0	21
7	Small-Area SAR ADCs With a Compact Unit-Length DAC Layout. IEEE Transactions on Circuits and Systems II: Express Briefs, 2022, 69, 4038-4042.	3.0	1
8	A 2.2 fJ/Conversion-Step 9.74-ENOB 10 MS/s SAR ADC With \$1.5×Input Range. IEEE Transactions on Circuits and Systems II: Express Briefs, 2022, 69, 3660-3664.	3.0	2
9	Printed Organic Electronics on Flexible Foil: Circuit Design and Emerging Applications. IEEE Transactions on Circuits and Systems II: Express Briefs, 2021, 68, 42-48.	3.0	9
10	A 1.25 μJ per Measurement Ultrasound Rangefinder System in 65 nm CMOS for Explorations With a Swarm of Sensor Nodes. IEEE Transactions on Circuits and Systems I: Regular Papers, 2021, 68, 1409-1420.	5.4	3
11	Analog and Mixed Signal Circuit Design Techniques in Flexible Unipolar a-IGZO TFT Technology: Challenges and Recent Trends. IEEE Open Journal of Circuits and Systems, 2021, 2, 743-756.	1.9	12
12	An RX AFE With Programmable BP Filter and Digitization for Ultrasound Harmonic Imaging. IEEE Transactions on Biomedical Circuits and Systems, 2021, 15, 1430-1440.	4.0	9
13	The Impact of the AFE BPF in Ultrasound Harmonic Imaging: An In-Vitro Phantom Study. , 2021, , .		1
14	A 0.38-pJ/b Simplex and a 1.2-pJ/b Full-Duplex Chip-to-Chip Digital Communication Interface With Data Rate and Load Capacitance Adaptability. IEEE Solid-State Circuits Letters, 2020, 3, 322-325.	2.0	0
15	A 2.67 μJ per Measurement FMCW Ultrasound Rangefinder System for the Exploration of Enclosed Environments. IEEE Solid-State Circuits Letters, 2020, 3, 326-329.	2.0	4
16	A 2.18-pJ/conversion, 1656- <i>μ</i> m² Temperature Sensor With a 0.61-pJ·K² FoM and 52-pW Stand-By Power. IEEE Solid-State Circuits Letters, 2020, 3, 82-85.	2.0	19
17	A Compact Fully Dynamic Capacitance-to-Digital Converter With Energy-Efficient Charge Reuse. IEEE Solid-State Circuits Letters, 2020, 3, 514-517.	2.0	7

18 Printed Smart Sensing Surfaces: technology, design and applications. , 2019, , .

1

EUGENIO CANTATORE

#	Article	IF	CITATIONS
19	A Gravure-Printed Organic TFT Technology for Active-Matrix Addressing Applications. IEEE Electron Device Letters, 2019, 40, 1682-1685.	3.9	20
20	A 0.1-nW–1-\$mu\$ W Energy-Efficient All-Dynamic Versatile Capacitance-to-Digital Converter. IEEE Journal of Solid-State Circuits, 2019, 54, 1841-1851.	5.4	31
21	A â^'81.6dBm Sensitivity Ultrasound Transceiver in 65nm CMOS for Symmetrical Data-Links. , 2019, , .		2
22	The Impact of Analog Front-end Filters on Ultrasound Harmonic Imaging. , 2019, , .		3
23	A 0.34-571nW All-Dynamic Versatile Sensor Interface for Temperature, Capacitance, and Resistance Sensing. , 2019, , .		19
24	Dynamic Output Resistance Optimization for Duty-cycle Control in Hybrid Capacitive LED Drivers. , 2018, , .		0
25	Organic Pressure-Sensing Surfaces Fabricated by Lamination of Flexible Substrates. IEEE Transactions on Components, Packaging and Manufacturing Technology, 2018, 8, 1159-1166.	2.5	10
26	A Fully Integrated 11.2-mm ² a-IGZO EMG Front-End Circuit on Flexible Substrate Achieving Up to 41-dB SNR and 29-M\$Omega\$ Input Impedance. IEEE Solid-State Circuits Letters, 2018, 1, 142-145.	2.0	24
27	Dimmable integrated CMOS LED driver based on a resonant DC/DC hybridâ€switched capacitor converter. International Journal of Circuit Theory and Applications, 2018, 46, 1485-1502.	2.0	4
28	A 93.3% Peak-Efficiency Self-Resonant Hybrid-Switched-Capacitor LED Driver in 0.18- <inline-formula> <tex-math notation="LaTeX">\$mu\$ </tex-math> </inline-formula> m CMOS Technology. IEEE Journal of Solid-State Circuits, 2018, 53, 1924-1935.	5.4	3
29	A 174 pW–488.3 nW 1 S/s–100 kS/s All-Dynamic Resistive Temperature Sensor With Speed/Resolution/Resistance Adaptability. IEEE Solid-State Circuits Letters, 2018, 1, 70-73.	2.0	48
30	Design of a Low-power Ultrasound Transceiver for Underwater Sensor Networks. , 2018, , .		4
31	Unified Physical DC Model of Staggered Amorphous InGaZnO Transistors. IEEE Transactions on Electron Devices, 2017, 64, 1076-1082.	3.0	7
32	Introduction to the Special Issue on the 46th European Solid-State Circuits Conference (ESSCIRC). IEEE Journal of Solid-State Circuits, 2017, 52, 1700-1702.	5.4	0
33	Exploring the unknown through successive generations of low power and low resource versatile agents. , 2017, , .		6
34	Ambipolar Organic Triâ€Gate Transistor for Lowâ€Power Complementary Electronics. Advanced Materials, 2016, 28, 284-290.	21.0	39
35	A 0.20 \$ext {mm}^2\$ 3 nW Signal Acquisition IC for Miniature Sensor Nodes in 65 nm CMOS. IEEE Journal of Solid-State Circuits, 2016, 51, 240-248.	5.4	95
36	Ultra-high gain diffusion-driven organic transistor. Nature Communications, 2016, 7, 10550.	12.8	54

EUGENIO CANTATORE

#	Article	IF	CITATIONS
37	An Integrated 13.56-MHz RFID Tag in a Printed Organic Complementary TFT Technology on Flexible Substrate. IEEE Transactions on Circuits and Systems I: Regular Papers, 2015, 62, 1668-1677.	5.4	112
38	A Low-Voltage Chopper-Stabilized Amplifier for Fetal ECG Monitoring With a 1.41 Power Efficiency Factor. IEEE Transactions on Biomedical Circuits and Systems, 2015, 9, 237-247.	4.0	93
39	Unified drain-current model of complementary p- and n-type OTFTs. Organic Electronics, 2015, 22, 5-11.	2.6	34
40	Positive-Feedback Level Shifter Logic for Large-Area Electronics. IEEE Journal of Solid-State Circuits, 2014, 49, 524-535.	5.4	49
41	11.1 An oversampled 12/14b SAR ADC with noise reduction and linearity enhancements achieving up to 79.1dB SNDR. , 2014, , .		70
42	High-Gain Operational Transconductance Amplifiers in a Printed Complementary Organic TFT Technology on Flexible Foil. IEEE Transactions on Circuits and Systems I: Regular Papers, 2013, 60, 3117-3125.	5.4	58
43	A 155 /spl mu/W 88-dB DR Discrete-Time /spl Delta/ /spl Sigma/ Modulator for Digital Hearing Aids Exploiting a Summing SAR ADC Quantizer. IEEE Transactions on Biomedical Circuits and Systems, 2013, 7, 573-582.	4.0	17
44	A 10b/12b 40 kS/s SAR ADC With Data-Driven Noise Reduction Achieving up to 10.1b ENOB at 2.2 f]/Conversion-Step. IEEE Journal of Solid-State Circuits, 2013, 48, 3011-3018.	5.4	163
45	A Power-Optimal Design Methodology for High-Resolution Low-Bandwidth SC \$DeltaSigma\$ Modulators. IEEE Transactions on Instrumentation and Measurement, 2012, 61, 2896-2904.	4.7	13
46	Charge Transport in Organic Transistors Accounting for a Wide Distribution of Carrier Energies—Part II: TFT Modeling. IEEE Transactions on Electron Devices, 2012, 59, 1520-1528.	3.0	44
47	Transport Physics and Device Modeling of Zinc Oxide Thin-Film Transistors Part I: Long-Channel Devices. IEEE Transactions on Electron Devices, 2011, 58, 2610-2619.	3.0	91
48	Transport Physics and Device Modeling of Zinc Oxide Thin-Film Transistors—Part II: Contact Resistance in Short Channel Devices. IEEE Transactions on Electron Devices, 2011, 58, 3025-3033.	3.0	30
49	Impact of energetic disorder and localization on the conductivity and mobility of organic semiconductors. , 2011, , .		2
50	Ordered Semiconducting Self-Assembled Monolayers on Polymeric Surfaces Utilized in Organic Integrated Circuits. Nano Letters, 2010, 10, 1998-2002.	9.1	37
51	Bottom-up organic integrated circuits. Nature, 2008, 455, 956-959.	27.8	366
52	High-performance organic integrated circuits based on solution processable polymer-small molecule blends. Applied Physics Letters, 2008, 93, .	3.3	74
53	Organic complementary-like inverters employing methanofullerene-based ambipolar field-effect transistors. Applied Physics Letters, 2004, 85, 4205-4207.	3.3	179
54	Flexible active-matrix displays and shift registers based on solution-processed organic transistors. Nature Materials, 2004, 3, 106-110.	27.5	1,516

#	ARTICLE	IF	CITATIONS
55	Polymer-based transistors used as pixel switches in active-matrix displays. Journal of the Society for Information Display, 2002, 10, 195.	2.1	18